Croatian Society for Materials Protection

Metalurgija/Metallurgy

Vol. 65 No. 4 / 2026

Staged Improvement of Technological Efficiency in FeSi75 Production in a Six-Electrode Submerged Arc Furnace

Sławomir Kozłowski [1]*, Radosław Miśkiewicz [2], Wojciech Bialik [3], Stanisław Gil [3], and Tomasz Kraszewski [3]

https://doi.org/10.64486/m.65.4.12

[1] Re Alloys sp. z o.o., Łaziska Górne, Poland; slawomir.kozlowski@realloys.pl
[2] University of Szczecin, Szczecin, Poland; radoslaw.miskiewicz@usz.edu.pl
[3] Silesian University of Technology, Gliwice, Poland; wojciech.bialik@polsl.pl, stanislaw.gil@polsl.pl, tomasz.kraszewski@polsl.pl
* Correspondence: slawomir.kozlowski@realloys.pl

Type of Paper: Article
Received: February 27, 2026
Accepted: April 17, 2026

Abstract: The production of high-silicon alloys in submerged arc furnaces (SAFs) is among the most energy-intensive processes in ferroalloy metallurgy. This paper reports a staged improvement of technological efficiency during industrial FeSi75 production in a six-electrode SAF. Performance was assessed using daily productivity, specific electricity consumption, and stability of silicon content in the product. The analysis used daily production records (electricity and product mass aggregated over 24 h; chemical composition calculated as a mass-weighted average of product containers). Shutdown and start-up days were excluded using current- and power-based criteria. In 2020, the structure of carbon reductants was modified, which coincided with a decrease in specific electricity consumption by approximately 120 kWh/Mg relative to 2016–2019. In 2023, the bath depth was reduced from 2500 mm to 2200 mm, and the operating point was intensified (active power from 5.7 MW to 6.1 MW; electrode current from 28 kA to 31 kA), resulting in a further reduction in specific electricity consumption and an increase in daily productivity. Throughout the analysed period, the silicon content remained stable at about 75 wt. % Si. In the investigated stage, the power-supply system (transformers and short network) was not modernised, indicating that measurable KPI improvements can be achieved through process- and construction-side actions and operating-regime optimisation under industrial constraints.

Keywords: ferrosilicon; FeSi75; submerged arc furnace (SAF); six-electrode furnace; specific electricity consumption; productivity; carbon reductants

1. Introduction

High-silicon ferroalloys produced in submerged arc furnaces (SAFs) exhibit high energy and material intensity. This is primarily due to the carbothermic reduction of silica, which requires temperatures on the order of (1800–2000) °C, and the need to heat large masses of burden and products to these temperatures. Producing 1 Mg of FeSi75 typically involves processing several tonnes of raw materials, including oxide materials (e.g., quartzite and iron oxides) and carbonaceous reductants, which translates into substantial consumption of electrical energy and the chemical energy of reductants [1–3].

In recent years, the European ferroalloy industry has operated under strong cost pressure driven by electricity prices, raw-material costs, and competition from producers outside the EU [4]. For ferrosilicon smelting,

electricity is the dominant cost component and often constitutes a major share of total production cost [1,2]. Therefore, improving technological efficiency – understood here as lowering specific electricity consumption while maintaining alloy quality and high productivity – remains a key development direction for SAF operation [5,6]. From a management perspective, such efficiency-driven process improvements align with the Industry 4.0 paradigm, wherein continuous monitoring, data-driven KPI assessment, and staged operational adjustments replace capital-intensive modernisation as the primary pathway to competitiveness in energy-intensive manufacturing [4–6].

The use of six-electrode furnaces in slag-free processes such as FeSi smelting is challenging. In slag-forming processes, the liquid slag phase helps stabilise bath resistance and the temperature field. In contrast, slag-free FeSi smelting is local in nature: reaction zones form beneath each electrode, and the energy input to each zone depends on arc–resistance conditions. As a result, electrode load asymmetry and losses in the power-supply system may reduce thermal stability and increase energy consumption [1,2,7–10].

The objective of this study is to present staged actions that improved the technological efficiency of a six-electrode SAF during FeSi75 production. Efficiency is evaluated in terms of specific electricity consumption, daily productivity, and stability of silicon content. In the analysed period, no modernisation of the power-supply system (transformers and short network) was implemented; the observed improvements result from process- and construction-side measures and a change in the furnace operating point.

2. Methodology and definitions of technological efficiency indicators

Technological efficiency was assessed using three indicators: daily productivity, specific electricity consumption, and alloy quality (silicon content). In addition, continuous recording of electrode/phase currents was used to evaluate electro-thermal operating conditions and electrode load stability.

Daily productivity Q_d was defined as the mass of ferrosilicon produced and transported from the furnace within one day (24 h). Product mass was controlled using a certified truck scale at the point of dispatch from the melt shop.

Specific electricity consumption E_{sp} was calculated as the ratio of the electricity E consumed in the analysed period [kWh] to the mass of alloy m produced in the same period [Mg]. E_{sp} is reported in [kWh/Mg].

Electricity consumption was recorded using certified electricity meters installed at the Main Power Supply Station feeding the furnace. In this study, E and m were aggregated daily (24 h) according to production records.

Alloy quality was evaluated based on silicon content (wt. % Si). Metal samples were taken from each tapping, i.e., typically 12 times per day. Metal from four consecutive tappings was directed to a single container. After preliminary crushing of the material in the container, a representative sample was taken, then ground, homogenised, and pressed into a pellet for analysis.

Chemical composition was determined in the plant laboratory by X-ray fluorescence (XRF) using a Thermo Fisher Scientific ARL PERFORM X 4200 spectrometer.

Daily silicon content in the alloy was calculated as a mass-weighted average based on the FeSi75 mass in individual containers dispatched from the furnace for further processing.

Phase currents were measured continuously and reported at 1 s intervals (1 Hz) with a resolution of 0.01 kA. Rogowski coils were installed on conductive parts of the power-supply system on the secondary side of the furnace transformers and connected to a dedicated hardware–software platform for data acquisition and storage.

Due to planned furnace shutdowns in industrial practice (e.g., during periods of high electricity prices), current-based stability metrics were evaluated only for operating days. A day was classified as an operating day if the mean electrode current was 25 kA and the active power exceeded 0.8 of nominal power.

https://doi.org/10.64486/m.65.4.12

3. Specificity of FeSi75 smelting in a six-electrode furnace and main sources of losses

The object of the study is Furnace XVI, a SAF commissioned in 1952 for ferrosilicon production. It is an open, low-shaft furnace with automatic electrode control and the possibility of manual control. The furnace is equipped with a rectangular bath, six Søderberg self-baking electrodes of 900 mm diameter arranged quasi-linearly in two opposing rows, and two tap-holes located on opposite sides of the furnace (Figure 1).

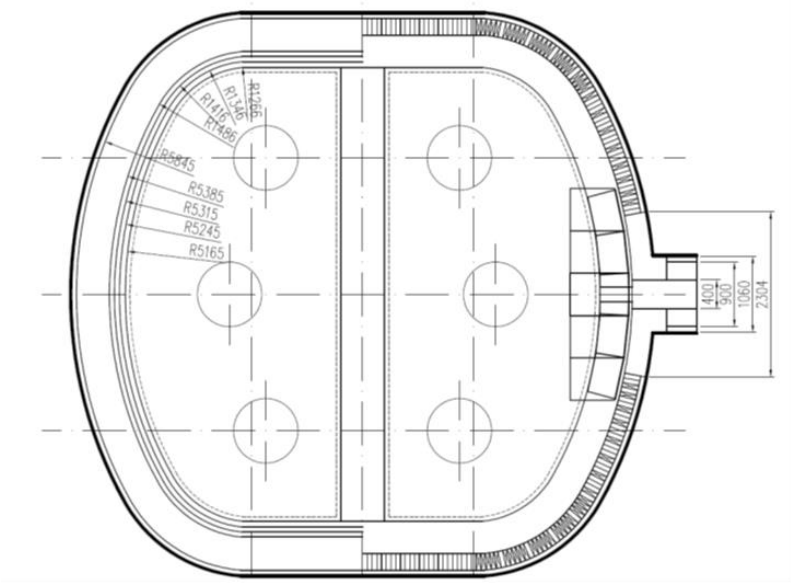

Figure 1. Plan view of Furnace XVI (six-electrode layout)

Furnace XVI is equipped with two transformers of 7.75 MVA rated power. Their parameters are listed in table 1.

Table 1. Furnace transformer parameters

Tap no.	Power kVA	Primary current/A	Primary voltage/V	Secondary current/A	Secondary voltage/V
1	7750	722.0	6200	29600	151.2
2	6970	646.0	6200	29600	136.0
3	6330	590.0	6200	29600	123.5
4	5790	539.0	6200	29600	113.0
5	5330	497.0	6200	29600	104.2
6	4970	462.5	6200	29600	97.0

A large voltage step between consecutive transformer taps and the lack of on-load tap changing prevent smooth control of the electrical regime of Furnace XVI and disturb the technological course of reductive smelting. In addition, the short network of Furnace XVI is relatively long, which causes significant losses between the electrical energy supplied to the furnace and the energy delivered from the transformer; these losses average 17 %. Under real conditions, supply-system asymmetry results in non-uniform thermal conditions among electrodes, associated with different electrode tip positions in the furnace and the presence of a so-called “dead phase”. Moreover, the electrode suspension and regulation system has an obsolete design: the electrode supporting cylinder is suspended on two hoist ropes driven by a worm-gear reducer, which may lead to electrode tilt due to uneven rope motion, wear, or uneven charge distribution. Directional shifts of electrodes in the bath change the pitch circle diameter and disturb the electrical and technological regime of ferrosilicon smelting. In addition, the system exhibits high inertia and a relatively large electrode stroke.

https://doi.org/10.64486/m.65.4.12

However, in addition to the obvious shortcomings resulting from 1950s construction solutions, lack of major modernisation, and the spatial/structural constraints of the melt shop building in which Furnace XVI operates, the furnace also has several advantages. In particular, six-electrode furnaces provide a more favourable distribution of heat generated by current flow and more advantageous temperature conditions in reaction zones, which partly compensates for high losses in the supply system.

Figure 2 shows a 3D model of Furnace XVI. Based on an electric-field and temperature-field distribution model developed by researchers from the Silesian University of Technology, calculated results for Furnace XVI are presented: internal temperature distribution (Figure 3) and temperature distribution on the outer surface of the furnace shell (Figure 4).

3.1. Model assumptions and limitations

Although Furnace XVI is supplied with AC, due to the low frequency (50 Hz) the electrical field was approximated using a DC formulation. The coupled fields were described by the Laplace equation for the electric potential and the Fourier–Kirchhoff heat-conduction equation with volumetric Joule heat generation, supplemented by an additional term representing the heat demand of endothermic reactions. The 3D non-linear problem was solved using the finite element method. Thermophysical and electrical properties of the burden, electrodes and lining were treated as effective properties (primarily temperature-dependent); conductivity data in the lower-temperature range were based on literature/empirical inputs and extrapolated at higher temperatures, while the effective thermal conductivity of the burden was estimated from constituent data using a mass-weighted approach. Boundary conditions included prescribed electric potential and temperature in the electrode contact region, grounding at the carbon blocks of the furnace lining, convective heat transfer on external surfaces, and continuity conditions at interfaces. Given these assumptions and the steady-state character of the calculations (no explicit transient tapping/start-up effects and no explicit burden heterogeneity), the model is used in this paper mainly for qualitative/comparative interpretation of how electrode position and bath/lining geometry affect the temperature distribution, rather than for exact prediction of absolute temperatures during transient industrial operation.

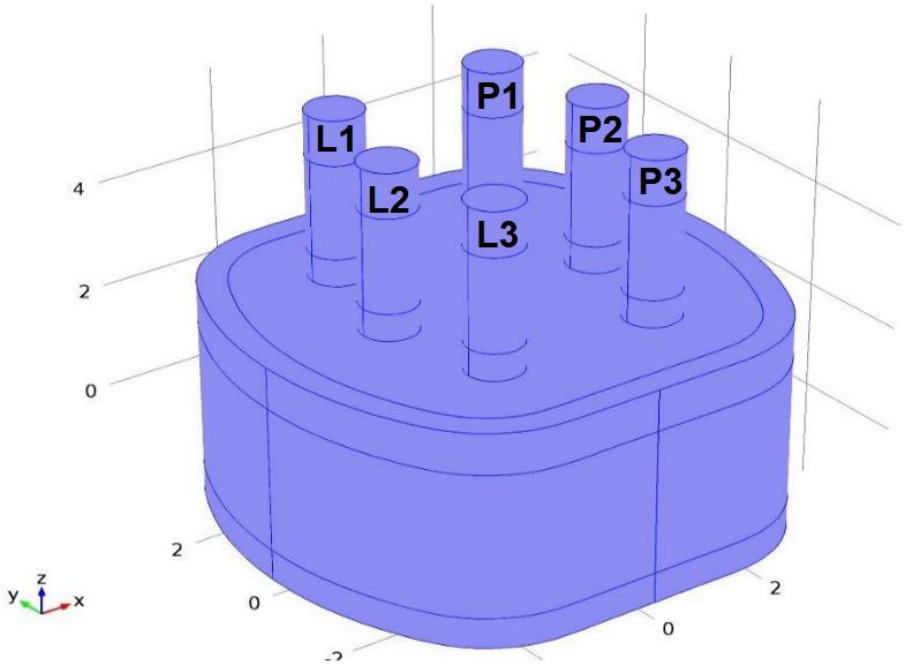

Figure 2. Geometric 3D model of Furnace XVI [12]

https://doi.org/10.64486/m.65.4.12

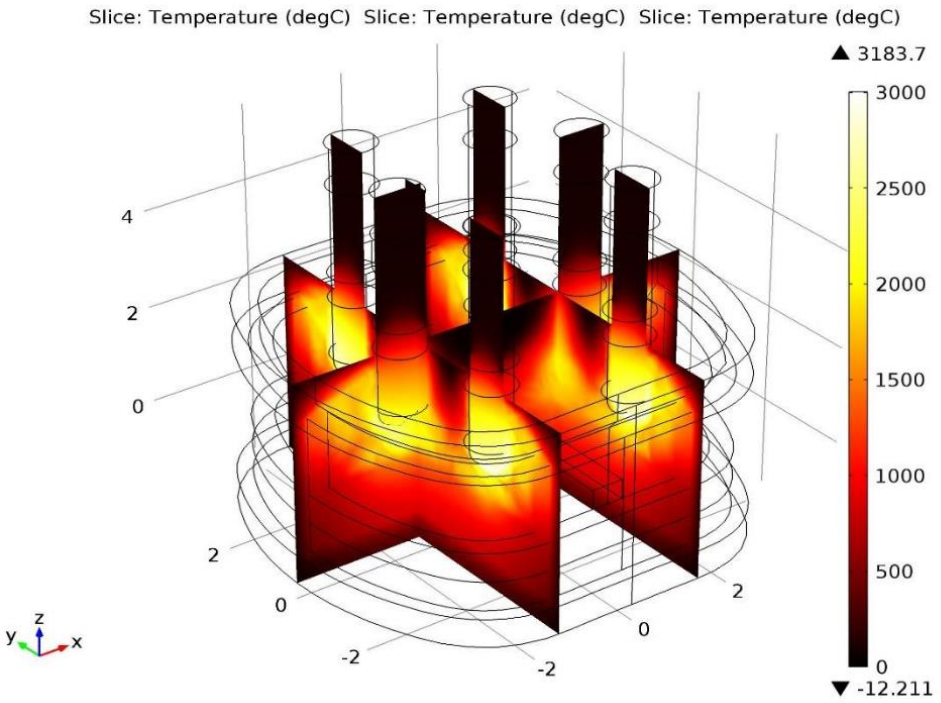

Figure 3. Temperature field in reaction zones around Furnace XVI electrodes [12]

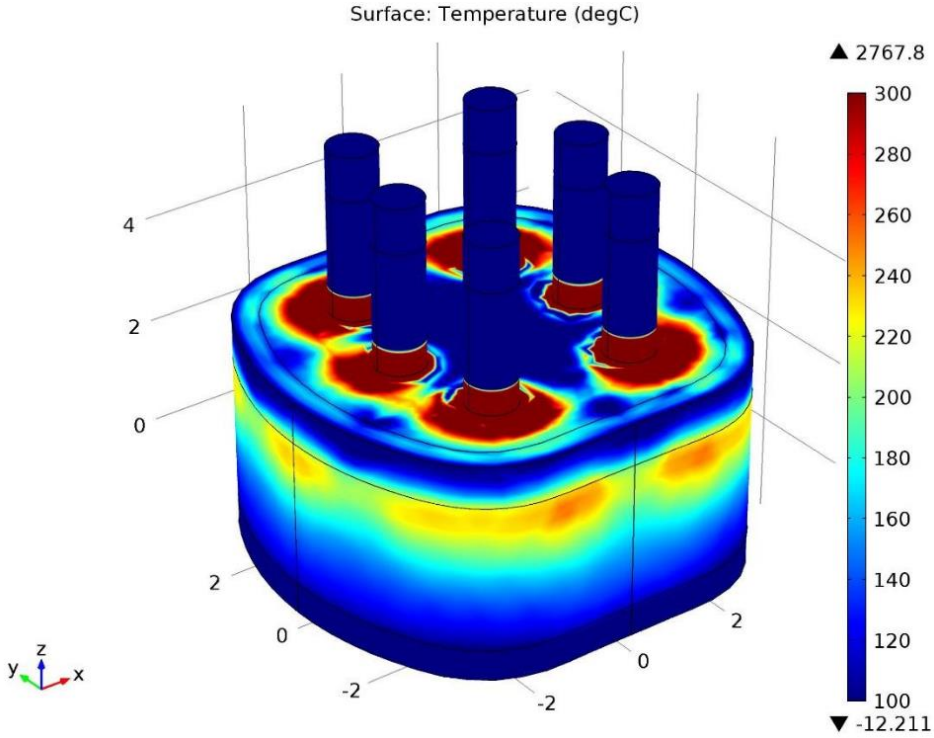

Figure 4. Temperature field on the external surface of Furnace XVI shell [12]

Notably, the two middle electrodes (L2, P2—Figure 2), positioned opposite the tap-holes, exhibit current density concentrated near their tips, while only a small portion of side-surface current is directed through the carbon lining of the side wall. In a circular furnace, the interaction area between the carbon lining and the electrode electric field is much larger; with an excessively high carbon lining, heat generation in the upper furnace zones may be too high. This leads to overly high temperatures in the upper zones and unfavourable conditions for SiO condensation, which adversely affects Si recovery [1,8,13,14].

 https://doi.org/10.64486/m.65.4.12

In slag-free FeSi smelting, local reaction zones form beneath each electrode. Thermal energy originates from arc radiation and from Joule heating in the conducting burden. The overall process rate is the sum of the rates in individual electrode zones and in the regions between electrodes [15]. Thus, non-uniform power input to electrodes may result in different reduction conditions and reduced process stability [1,7,9,10].

In the overall energy balance, processes occurring in the furnace bath dominate. However, a significant share of energy is also consumed by losses in the power-supply system between the transformer primary side and the electrodes, and by auxiliary installations (gas extraction/dedusting, cooling) [16]. Reducing useful-energy losses to the bath and stabilising conditions in electrode reaction zones are therefore crucial for improving E_{sp} and productivity [2,11].

4. Implemented actions and change of the furnace operating point

Re Alloys' technology department was aimed at improving the efficiency of FeSi75 production in Furnace XVI without modernising the power-supply system (transformer connection configuration and short-network geometry remained unchanged). Due to infrastructural constraints and the need to limit investment intervention, the work focused on process- and construction-side actions that could be implemented without rebuilding the power-supply system. The primary target was to reduce the average specific electricity consumption from 8850 kWh/Mg to 8650 kWh/Mg, increase daily productivity from 28.5 Mg to 31 Mg, while maintaining Si content ≥75 wt. %.

4.1. Change in the carbon reductant structure (2020)

In 2020, the structure of carbon reductants used in the process was modified to improve the course of carbothermic reactions and operating stability. The reductants are classified based on fixed carbon (C_{fix}). C_{fix}, in relation to reaction (1), enables determination of reductant demand expressed via the molar ratio C/SiO_2.

$$SiO_2 + 2C = Si + 2CO \quad (1)$$

In the as-received state, C_{fix} is calculated from proximate analysis parameters (2).

$$C_{fix} = 100 - W^r - A^r - V^r \quad (2)$$

Until 2020, the reductant structure (expressed as fixed-carbon contribution) was as follows: 70 % of Cfix originated from "Marcel" coal (volatile matter <30 %), 27 % from "Chwałowice" coal (volatile matter >30 %), and the remainder from wood chips. The coal parameters are given in Table 2.

Table 2. Proximate analysis of "Marcel" and "Chwałowice" coals

Coal	C_{fix}	W^r	V^r	A^r	Phosphorus
Marcel	64.0	3.2	29.6	3.2	0.0046
Chwałowice	52.7	7.6	35.1	4.6	0.1106

A key advantage of high-volatile reductants is their higher reactivity towards gases such as CO_2, H_2O, and SiO, and—depending on structure and particle size—their influence on the electrical properties of the burden [17]. High SiO reactivity is important for limiting silicon losses and improving Si recovery, which affects techno-economic indicators. Therefore, the share of coal with volatile matter above 30 % was intended to be increased [13,18–21].

However, the high phosphorus content of "Chwałowice" coal was problematic. Phosphorus largely transfers to the alloy, contaminating the product and increasing the tendency of ferrosilicon to self-disintegrate [22–24]. Therefore, tests with alternative coals were performed. In 2020, "Szubarkol" coal was introduced; its parameters are listed in Table 3.

Table 3. Proximate analysis of "Szubarkol" coal (wt. %)

Coal	C_{fix}	W^r	V^r	A^r	Phosphorus
Szubarkol	46.6	12.4	35.0	6.0	0.0337

https://doi.org/10.64486/m.65.4.12

The substantially lower phosphorus content of "Szubarkol" compared with "Chwałowice" allowed an increased share of high-volatile coal in the charge. After the change, 49 % of C_{fix} originated from "Marcel" (VM <30 %), 48 % from "Szubarkol" (VM >30 %), and the remainder from wood chips. Industrial practice indicates that higher volatile matter and moisture content promote intense gas release during heating, which develops porosity and specific surface area and thus increases reductant reactivity [19,21,25].

Literature on carbonaceous materials shows that higher porosity can improve performance in high-temperature processes, as porosity is a key technological property alongside reactivity and resistivity [19,21,26,27]. At the same time, more pores may worsen grain-to-grain contact in the bed and increase contact resistance, thereby increasing the electrical resistivity of the burden layer [27–31].

This is beneficial in SAF operation, because burden resistivity influences current distribution and the conditions in electrode reaction zones and therefore thermal stability [1,7,10,32]. Moreover, appropriate reductant selection (structure, porosity, electrical properties) may improve process efficiency and reduce specific electricity consumption in FeSi production [20,32–34].

After changing the reductant structure, specific electricity consumption decreased by approximately 120 kWh/Mg on average.

4.2. Bath geometry modification and increased electrical parameters (2023)

In 2023, during furnace maintenance, a decision was made to reduce the bath depth from 2500 mm to 2200 mm and to correspondingly reduce the height of the carbon lining. The objective was to improve utilisation of the working volume and thermal conditions in reaction zones.

Model calculations [12] indicate that a lower carbon-lining height requires deeper electrode immersion to reach the target current load and phase power and simultaneously leads to a more favourable temperature distribution from the viewpoint of the physicochemical process. This is associated with higher temperatures near electrode tips and lower burden temperatures in the upper furnace zones [1,7,10].

Despite simplifications, the model [12] satisfactorily captures the thermal conditions inside the furnace bath and helps explain relationships among electrical parameters, electrode position, and process temperature conditions.

For fixed burden properties and a fixed burden level, increasing current load is associated with deeper electrode immersion and a decrease in upper-zone temperatures [7,9,10]. Figures 5 and 6 show calculated temperature distributions for the deep and shallow bath configurations.

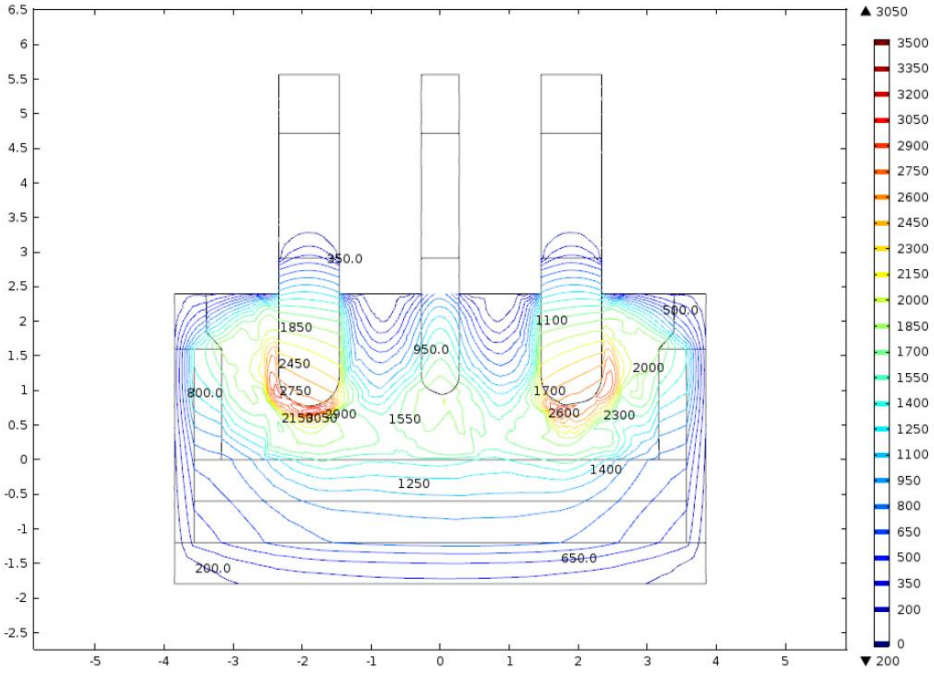

Figure 5. Temperature distribution in a section through electrodes P1–P3 with the deep bath [12]

 https://doi.org/10.64486/m.65.4.12

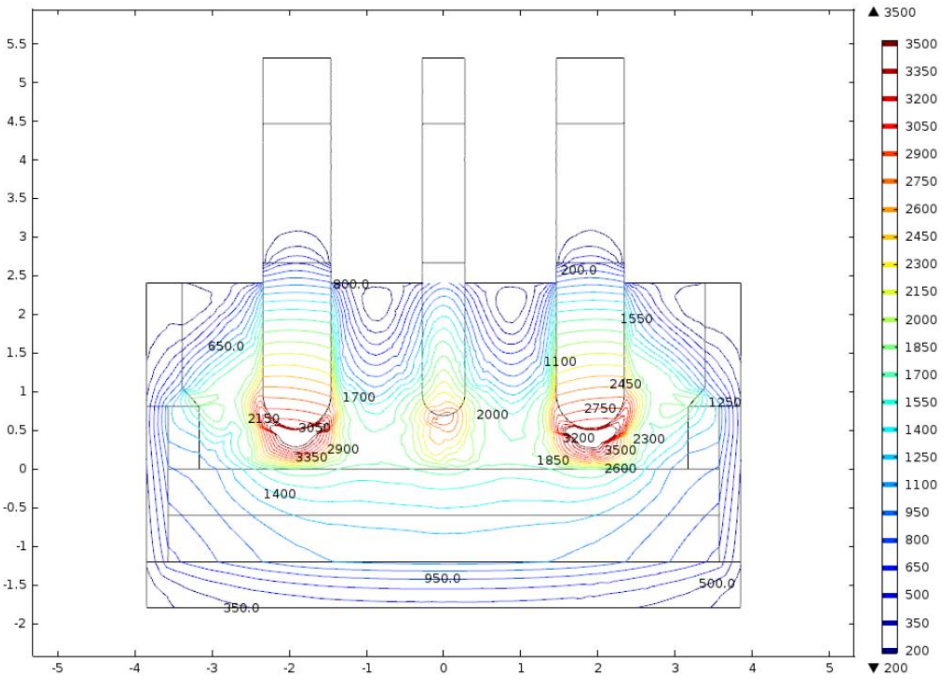

Figure 6. Temperature distribution in a section through electrodes P1–P3 after bath shallowing [12]

After implementing the bath-depth and carbon-lining changes, furnace operating parameters were improved: active power increased from ~5.7 MW to 6.1 MW and electrode current from ~28 kA to 31 kA. Due to deeper electrode immersion, conditions for SiO condensation in the upper burden layers improved. The change in operating point enabled a further decrease in the average specific electricity consumption to 8650 kWh/Mg and an increase in productivity to 31 Mg/day while maintaining Si content ≥75 wt. % Si.

5. Results and discussion

The implemented process and construction changes enabled achieving the planned target, as shown in Figure 7.

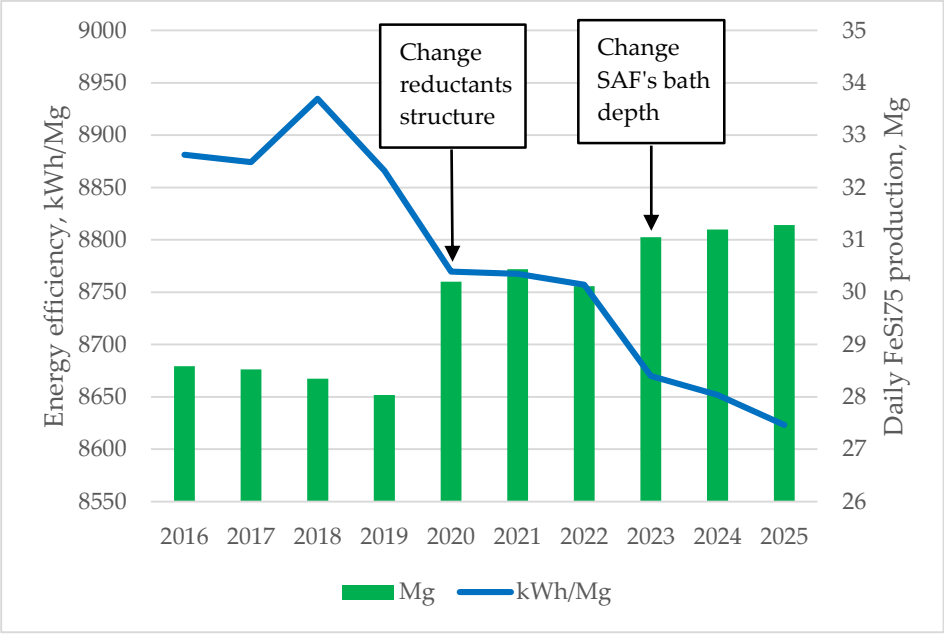

Figure 7. Annual changes in E_{sp} and Q_d

https://doi.org/10.64486/m.65.4.12

Table 4 summarises annual values of average daily productivity, Q_d(Mg/day), specific electricity consumption, E_{sp}[kWh/Mg], and the mass-weighted silicon content in the alloy (wt. %). Shutdown days with zero electricity consumption (E = 0 kWh) and start-up days after shutdowns were excluded from the analysis. A start-up day was defined as an operating day until the mean active power reached 0.8 of nominal power.

Table 4. Annual summary of average daily E_{sp}, Q_d and mass-weighted Si content for FeSi75

Year	E_{sp}/(kWh/Mg)	Q_d/Mg	Si/(wt. %)
2016	8881	28.58	75.28
2017	8874	28.52	75.21
2018	8935	28.35	74.98
2019	8866	28.03	75.35
2020	8770	30.20	75.42
2021	8768	30.44	74.65
2022	8757	30.12	75.42
2023	8670	31.05	75.36
2024	8652	31.20	75.37
2025	8623	31.28	75.38

Further increases in furnace productivity are constrained by the current tapping/receiving system, which limits the volume of metal per tapping. Further reductions in specific electricity consumption may require modernisation of the power-supply system, particularly the transformers and short network.

The first improvement stage (2020) was primarily associated with changes in reductant quality/structure, which likely enhanced SiO reactivity and burden electrical/physical properties, resulting in an average reduction of E_{sp} by approximately 120 kWh/Mg. The second stage (2023) combined bath-geometry modification with an intensified operating point; the model indicates a more favourable temperature distribution (higher temperatures near electrode tips and lower temperatures in the upper zones), which likely improved conditions for SiO condensation/reaction and enabled operation at higher current and power, with a further reduction in E_{sp} and an increase in Q_d.

Limitations: The analysis is based on industrial production data collected under routine operating conditions rather than controlled experiments. Consequently, variability in raw materials and operational disturbances may influence the calculated KPIs. Moreover, some changes were implemented simultaneously (especially in 2023), which limits the possibility of quantitatively isolating the contribution of each individual measure. Therefore, the results should be interpreted as an industrial-scale assessment of KPI trends and their plausible technological drivers rather than a strictly causal attribution.

6. Conclusions

• Over 2016–2025, a gradual improvement in the energy intensity of FeSi75 smelting in the six-electrode furnace was observed: specific electricity consumption decreased from 8881 kWh/Mg in 2016 to 8623 kWh/Mg in 2025, while Si content remained stable at ~75 wt. % Si.

• The first improvement stage (2020), associated with changes in the carbon reductant structure, reduced specific electricity consumption by ~120 kWh/Mg relative to 2016–2019 without lowering Si content.

• The second improvement stage (2023), including bath-geometry modification (from 2500 mm to 2200 mm) and a shift in the operating point (active power from 5.7 MW to 6.1 MW; electrode current from 28 kA to 31 kA), enabled further reduction of E_{sp} and increased daily productivity while maintaining required alloy quality.

https://doi.org/10.64486/m.65.4.12

• No modernisation of the power-supply system was implemented in the analysed period, indicating that measurable KPI improvements can be achieved through staged process- and construction-side actions and operating-regime optimisation under existing infrastructure constraints.
• The methodology based on daily aggregation of production data (mass, energy, composition) and exclusion of shutdown and start-up days using current- and power-based criteria enables comparable KPI assessment under industrial conditions, including periodic shutdowns driven by economic factors.
• Further improvements may require measures beyond bath geometry and operating regime (e.g., operational constraints related to tapping/casting and, in subsequent stages, modernisation of power-supply components).

Acknowledgments: This paper is published with the permission of the Re Alloys sp. z o.o. Ferroalloys Plant management. The study is part of the project "Maximisation of energy efficiency in a six-electrode electric arc resistance furnace for high-content silicon alloys by developing innovative solutions, especially for the furnace power supply system", co-funded by the Polish NCBiR Committee, No. POIR.01.01.01-00-0938/17 within the Smart Growth Operational Programme 2014–2020.

References

[1] M. Gasik, Ed., Handbook of Ferroalloys: Theory and Technology, Oxford, UK: Elsevier/Butterworth-Heinemann, 2013, https://doi.org/10.1016/C2011-0-07613-6

[2] M. Gasik, V. Dashevskii, and A. Bizhanov, Ferroalloys: Theory and Practice. Cham, Switzerland: Springer Nature, 2020, https://doi.org/10.1007/978-3-030-57502-1

[3] A. Schei, J. K. Tuset, and H. Tveit, Production of High Silicon Alloys, Trondheim, Norway: Tapir Academic Press, 1998

[4] R. Miśkiewicz, A. Rzepka, R. Borowiecki, and Z. Olesiński, "Energy efficiency in the Industry 4.0 era: Attributes of teal organisations", *Energies*, vol. 14, no. 20, p. 6776, 2021, https://doi.org/10.3390/en14206776

[5] R. Miśkiewicz and R. Wolniak, "Practical application of the Industry 4.0 concept in a steel company", *Sustainability*, vol. 12, no. 14, p. 5776, 2020, https://doi.org/10.3390/su12145776

[6] R. Miśkiewicz, "Industry 4.0 in Poland – Selected Aspects of ITS Implementation", *Scientific Papers of Silesian University of Technology Organization and Management Series*, no. 136, pp. 403-413, 2019, http://dx.doi.org/10.29119/1641-3466.2019.136.31

[7] G. Sævarsdóttir and J. A. Bakken, "Current distribution in submerged arc furnaces for silicon metal / ferrosilicon production" in *Proceedings of the INFACON XII*, Helsinki, Finland, 2010, pp. 717–728

[8] G. Tranell, M. Andersson, E. Ringdalen, O. Ostrovski, and J. J. Steinmo, "Reaction zones in a FeSi75 furnace – results from an industrial excavation" in *Proceedings of the INFACON XII*, Helsinki, Finland, 2010

[9] G. Sævarsdóttir, T. Magnusson, and J. A. Bakken, "Electric arc on a coke bed in a submerged arc furnace" in *Proceedings of the INFACON XI*, New Delhi, India, 2007, pp. 572–582

[10] B. Bowman and K. Krüger, Arc Furnace Physics. Düsseldorf, Germany: Verlag Stahleisen GmbH, 2009

[11] Y. Toulouevski and I. Zinurov, Innovation in Electric Arc Furnaces. Berlin, Germany: Springer-Verlag, 2010

[12] Politechnika Śląska, Sprawozdanie z pracy naukowo-badawczej, Gliwice, Poland, Nov. 24, 2017 (unpublished internal report)

[13] T. Lindstad, S. Gaal, S. Hansen, and S. Prytz, "Improved SINTEF SiO-reactivity test" in *Proceedings of the INFACON XI*, New Delhi, India, 2007

[14] E. Ringdalen, G. Tranell, and O. Ostrovski, "Condensate in the metallurgical silicon process", *Metallurgical and Materials Transactions B*, vol. 42, no. 5, pp. 1066–1074, 2011, https://doi.org/10.1007/s11663-011-9528-9

[15] S. Gil, J. Góral, J. Ochman, M. Saternus, and W. Bialik, "An experimental study on the air delivery and gas removal method in a model of furnace for ferroalloy production" *Metalurgija*, vol. 53, no. 4, pp. 489–492, 2014

[16] V. P. Karasyov et al., "Iron loss in high-power arc steelmaking furnaces" *Metalurgija*, vol. 55, no. 3, pp. 379–382, 2016.

[17] W. Bialik, M. Saternus, S. Gil, and J. Ochman, "Properties of carbonaceous materials used in ferroalloy production" *Metalurgija*, vol. 52, no. 2, pp. 185–188, 2013

[18] S. E. Olsen, M. Tangstad, and T. Lindstad, "Reaction mechanisms of charcoal and coke in the silicon process" *ISIJ International*, vol. 40, no. 2, pp. 101–107, 2000

[19] M. Tangstad and S. E. Olsen, "Reductant characterisation and selection," in *Proceedings of the INFACON X*, Cape Town, South Africa, 2004

[20] S. E. Olsen, M. Tangstad, and T. Lindstad, "Coal in production of FeSi" in *Proceedings of the INFACON IX*, Québec City, Canada, 2001

[21] R. J. Gray and E. Liptakova, "Coal petrography and mineralogical study of reductants for ferroalloy production", *Fuel*, vol. 76, no. 2, pp. 181–190, 1997

[22] J. A. Bakken, E. Ringdalen, and G. Sævarsdóttir, "Effects of raw material contaminants on the ferrosilicon melting process in the submerged arc furnace," in *Proceedings of the INFACON XII*, Helsinki, Finland, 2010

[23] G. Tranell, E. Ringdalen, and O. Ostrovski, "Controlled solidification of ferrosilicon", in *Proceedings of the INFACON XIV*, Kyiv, Ukraine, 2015

[24] M. Tangstad and S. E. Olsen, "Effect of the structure of ferrosilicon on its disintegration", *Metallurgical and Materials Transactions B*, vol. 44, no. 4, pp. 943–952, 2013, https://doi.org/10.1007/s11663-013-9873-5

[25] E. Ringdalen and M. Tangstad, "Reductant moisture in FeSi75 production" in *Proceedings of the INFACON XIII*, Almaty, Kazakhstan, 2013

[26] O. Hjortland and S. E. Olsen, "Reactivity and conversion behaviour of biocarbon in silicon and ferrosilicon processes" *Energy Procedia*, vol. 20, pp. 125–132, 2012

[27] M. Saternus and W. Bialik, "Influence of carbon material structure on high-temperature metallurgical processes" *Metalurgija*, vol. 51, no. 4, pp. 453–456, 2012

[28] S. Gil and J. Ochman, "Behaviour of coke and coal in ferroalloy furnaces" *Metalurgija*, vol. 50, no. 3, pp. 189–192, 2011

[29] R. J. Gray and H. Marsh, "Resistivity of metallurgical coke" *Fuel*, vol. 65, no. 10, pp. 1440–1444, 1986

[30] R. Sundqvist and A. Jansson, "Influence of coke particle size on the electrical resistivity of the burden in submerged arc furnaces" *Scandinavian Journal of Metallurgy*, vol. 28, no. 4, pp. 181–187, 1999

[31] S. E. Olsen and M. Tangstad, "The behaviour of coke in submerged arc furnaces" in *Proceedings of the INFACON VIII*, Beijing, China, 1998

[32] W. Bialik, M. Saternus, and S. Gil, "Raw material selection and its influence on energy consumption in submerged arc furnaces" *Metalurgija*, vol. 54, no. 1, pp. 53–56, 2015

[33] S. E. Olsen, M. Tangstad, and T. Lindstad, "The importance of coal and coke in the production of ferrosilicon" in *Proceedings of the INFACON IX*, Québec City, Canada, 2001

[34] M. Tangstad, E. Ringdalen, and S. E. Olsen, "A more energy-efficient ferrosilicon process" in *Proceedings of the INFACON XI*, New Delhi, India, 2007

 https://doi.org/10.64486/m.65.4.12